

# Development of Innovative Accident Tolerant High Thermal Conductivity UO<sub>2</sub>-Diamond Composite Fuel Pellets

---

## Fuel Cycle

James Tulenko  
University of Florida

In collaboration with:  
None

Frank Goldner, Federal POC  
Kenneth McClellan, Technical POC



**Development of Innovative Accident Tolerant High Thermal  
Conductivity UO<sub>2</sub>-Diamond Composite Fuel Pellets**

**NEUP Final Progress Report**

**January 2016**

**PI: James Tulenko**  
**tulenko@ufl.edu**

**Co-PI: Ghatu Subhash**

**Graduate Assistants: Jhonathan Rosales, Zhichao Chen, Timothy Iroman, Bijan Nili.**

**DOE Award Number: DE-AC07-05ID14517**

## Background

The University of Florida (UF) evaluated a composite fuel consisting of  $\text{UO}_2$  powder mixed with diamond micro particles as a candidate as an accident tolerant fuel (ATF). The research group had previous extensive experience researching with diamond micro particles as an addition to reactor coolant for improved plant thermal performance. The purpose of this research work was to utilize diamond micro particles to develop  $\text{UO}_2$ -Diamond composite fuel pellets with significantly enhanced thermal properties, beyond that already being measured in the previous UF research projects of  $\text{UO}_2$  – SiC and  $\text{UO}_2$  – Carbon Nanotube fuel pins. UF is proving with the current research results that the addition of diamond micro particles to  $\text{UO}_2$  may greatly enhanced the thermal conductivity of the  $\text{UO}_2$  pellets producing an accident tolerant fuel. The Beginning of life benefits have been proven and fuel samples are being irradiated in the ATR reactor to confirm that the thermal conductivity improvements are still present under irradiation.

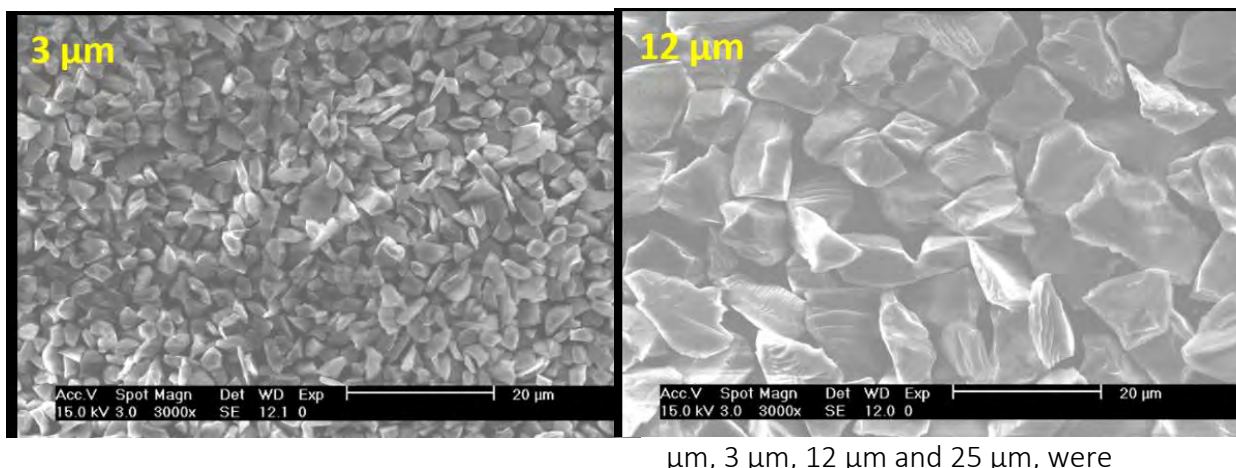
The diamond form of surface functionality allows for strong coupling with  $\text{UO}_2$  by formation of U-O-C surface bonding and therefore, enhanced thermal coupling to the  $\text{UO}_2$ . It is for this reason UF proposed  $\text{UO}_2$  pellets to be doped with Diamond micro particles. UF conducted a parametric study for  $\text{UO}_2$ +Diamond involving a range of volume fractions of Diamond (5%-15%), processing temperatures (900-1600 °C), pressures (30-80 MPa) and consolidation periods (3-15 min). The result was to identify the optimal volume fractions of Diamond and processing conditions that provided a well consolidated compact with optimal microstructure and enhanced thermal conductivity

As initially proposed, the fabrication of the  $\text{UO}_2$  –Diamond fuel was completed at the UF facilities by means of Spark Plasma Sintering (SPS). Under SPS processing rapid consolidation of the composite powder resulted in a dense microstructure with minimum grain growth. Using this technique, UF investigators successfully consolidated  $\text{UO}_2$ -Diamond composites up to a theoretical density of 98% with an enhanced thermal conductivity. UF has also developed excellent thermal etching methods to reveal the grain boundaries in our fuel composites. Finally, two capsules of  $\text{UO}_2$  –Diamond fuel samples with high density and commercial dimensions are undergoing irradiation tests at the Advanced Training Reactor (ATR) at Idaho National Laboratory. Upon completion of the tests UF will analyze the results to verify the  $\text{UO}_2$  –Diamond fuel performance under conditions expected in a reactor core.

$\text{UO}_2$ -diamond composites were fabricated using SPS and the densification evolution was studied. In addition, the micro structure and thermal properties of  $\text{UO}_2$ -diamond composite fuel were investigated thoroughly. Compared to other composite materials such as SiC or carbon-nanotubes, the suitability of diamond as a fuel dopant candidate was an unknown. Therefore, the objective of this work was to fabricate  $\text{UO}_2$ -diamond fuel pellets via SPS using different diamond particle sizes and investigate the microstructure and thermal properties to prove the industry and the NRC that the behavior of the fuel is well characterized and will not give unexpected results.

## Powder Preparation

The uranium dioxide powder was obtained from AREVA Federal Services, Hanford, Washington, USA. The powder was reported to have a bulk density of  $2.3\text{g/cm}^3$ , mean particle diameter of  $2.4\mu\text{m}$ . The O/U ratio was determined to be 2.11 using ASTM equilibration method. The diamond powder was obtained from Advanced Abrasives, Pennsauken, NJ. Four sizes of diamond particles with a mean particle size of 0.25



$\mu\text{m}$ , 3  $\mu\text{m}$ , 12  $\mu\text{m}$  and 25  $\mu\text{m}$ , were

Figure 1. SEM images of Diamond micro particles. Sizes 3  $\mu\text{m}$  and 12  $\mu\text{m}$ .

used in this study. Figure 1 Shows SEM images of the 3  $\mu\text{m}$  and 12  $\mu\text{m}$  Diamond micro particle sizes. A SPEX-8000 shaker was used to mix  $\text{UO}_2$  with diamond powder for 1 hour with a blending aid 2,3-Dihydroperfluoropentane. The use of a blending aid was proven to be effective and non-contaminative to the final powder.<sup>1</sup>

## Mixing Powder Samples

Numerous sample pellets were fabricated utilizing depleted uranium powder mixed with 12  $\mu\text{m}$  diamond particles at 10% by volume basis with a theoretical density of  $3.52\text{g/cm}^3$ . A common method to uniformly disperse the diamond particles into a ceramic matrix is with the use of milling equipment. A SPEX 8000 mill was used to disperse the 12  $\mu\text{m}$  nanoparticles into the  $\text{UO}_2$  powder. To improve the dispersion rate, a 40 mL suspension of decafluoropentane was added to the mixture. Then, it was placed inside a ceramic vial and milled for 60 minutes. The main objective of the milling process is to obtain a homogeneous dispersion of the diamond particles into the  $\text{UO}_2$  matrix.

## Spark Plasma Sintering

Different die and punch sizes were used to sinter the mixed powders. A thin graphite foil was inserted into a graphite die and then 5g of UO<sub>2</sub>+diamond mixture was poured into the die to fabricate a full size pellet. Graphite punches were used on either side of the die to hold the powder. The graphite foil prevents reaction between the powders and the die. A Dr. Sinter® SPS-1030 spark plasma system (SPS) machine was used to sinter the blended powder. The entire die assembly with powder and punches was placed in the SPS chamber. During sintering, a vacuum of less than 10 Pa was maintained in the chamber and the temperature was measured using a pyrometer that focused on the surface of the graphite die. A temperature ramp rate of 100°C/min was employed and the maximum sintering temperature was varied from 1300°C to 1600°C with a hold time of 5 minutes for various powder mixtures. An axial pressure of 40 MPa was applied when the maximum sintering temperature was reached, and the pressure was released when the cooling process started.

### Characterization Methods

Upon cooling to room temperature, the pellets were removed from the graphite dies. The density of each sintered pellet was measured by the Archimedes method and converted to a relative density. The theoretical density of the composite was then calculated by the rule of mixture. In the equation below  $\rho_c$  is the theoretical density of the composite,  $\rho_d$ ,  $V_d$  and  $\rho_{UO_2}$  are the density of diamond, volume fraction of diamond, and density of UO<sub>2</sub>, respectively.

$$\rho_c = \rho_d V_d + \rho_{UO_2} (1 - V_d) \quad (1)$$

X-ray diffraction (XRD) measurements were conducted to investigate the chemical reactions which may have occurred between UO<sub>2</sub> and diamond during the sintering process. As the detection limit of XRD is around 5wt% of chemical compounds and the short processing time of 5 minutes may not be enough to form reaction compounds at sufficient quantity, the volume fraction of diamond was increased to 70% in the composite for this specific study only. The mixing process and sintering procedures were the same as the other pellets. X-Ray diffraction patterns were recorded with a PANalytical X'Pert Powder® diffractometer at room temperature. The 2 $\theta$  angle was scanned from 20° to 80° with a step size of 0.005°. The software X'Pert HighScore Plus® was used for peak fitting. To characterize the microstructure of the sintered pellets, scanning electron microscopy (JEOL-6335L and FEI XL-40 FEG-SEM) was used. The secondary electron mode was chosen for the images and the accelerating voltage was varied between 10 to 15 KV.

The thermal conductivity of the sintered composite pellets was calculated using the following equation:

$$K_c = \alpha_{cp} \rho C \quad (2)$$

Where  $\alpha$  is the thermal diffusivity,  $cp$  is the specific heat and  $\rho C$  is the density of the composite.  $\alpha$  was measured at three different temperatures, i.e., 100°C, 500°C and 900°C, using a laser flash method (Anter Flashline®-3000). Specific heat was calculated using the Neumann-Kopp rule<sup>2</sup>:

$$cp = cd \cdot fd + cuo2 \cdot (1 - fd) \quad (3)$$

where  $cd$  and  $cuo2$  are the specific heat of diamond and  $UO_2$ , respectively, and  $fd$  is the weight fraction of diamond.

The Young's modulus was determined using the ultrasonic measurement method, an accurate and non-destructive technique. Using a pulser/receiver system (Model 5072PR, Olympus, Waltham, MA), both longitudinal velocity  $Vl$  and shear velocity  $Vs$  of the pellets were measured. The Young's modulus is then calculated by the following equation<sup>3</sup>:

$$\nu = \frac{1 - 2\left(\frac{Vs}{Vl}\right)^2}{2 - 2\left(\frac{Vs}{Vl}\right)^2} \quad (4)$$

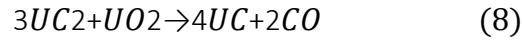
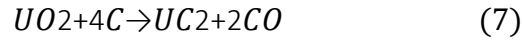
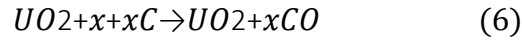
$$E = \frac{Vl^2 \cdot \rho(1 + \nu)(1 - 2\nu)}{1 - \nu} \quad (5)$$

Where  $\nu$  is Poisson's ratio,  $E$  is Young's modulus and  $\rho$  is the density of the pellet. Four measurements were performed on each composite and the average value was calculated.

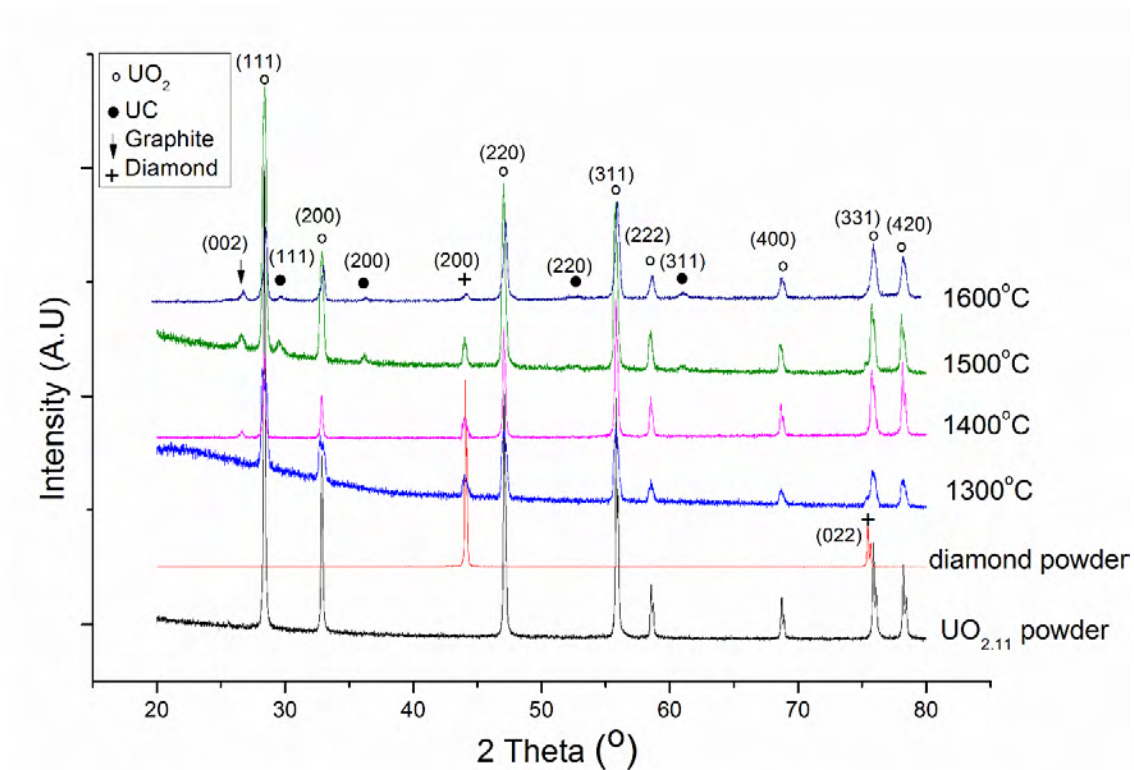
## Chemical Reaction – Graphitization of Diamond

Understanding the potential chemical reactions between diamond and  $UO_2$  during SPS is critical to an evaluation of the performance potential of the composite pellet in the reactor environment. The chemical reaction products, may badly influence the thermal and mechanical performance of the sintered pellets. Figure 2 shows the XRD spectra of  $UO_2$  and diamond powder as well as the  $UO_2$ -Diamond composite at four different temperatures. For the spectra of starting powders, all characteristic peaks of  $UO_2$  and diamond were clearly detected, revealing the cubic structure of  $UO_2$  and diamond. The crystal planes were identified and marked in the plot. For the  $UO_2$ -70 vol% diamond composite sintered at 1300°C, no other peaks, except  $UO_2$  and diamond peaks, were observed. However, when the maximum sintering temperature was increased to 1400°C, a clear graphite peak was detected. The formation of graphite may be an indication of the graphitization of diamond. Although it is known that the graphitization rate of diamond is extremely slow below 1600°C in an inert gas environment<sup>3</sup>, this temperature could decrease significantly if high pressure is applied. During SPS, a pressure of 40 MPa was applied at

the maximum sintering temperature, which could facilitate the graphitization process. When the maximum sintering temperature reached 1500°C or higher, not only graphite, but also uranium carbide (UC) peaks were observed. The following reactions between  $UO_2$  and carbon are expected<sup>4</sup>:



Note that there is CO gas formed in these reactions. Recall that slightly decrease in density was observed in pellets sintered at 1600°C, which may be due to the formation of gas. During the hold time at such high temperature, the sintering process was almost done, but some micro holes were left because of the formation of CO. The increase of porosity thus led to a decrease in final density. Clearly, higher sintering temperatures are not preferable due to the formation of graphite and other reaction products. Sintering temperatures well below 1500°C are



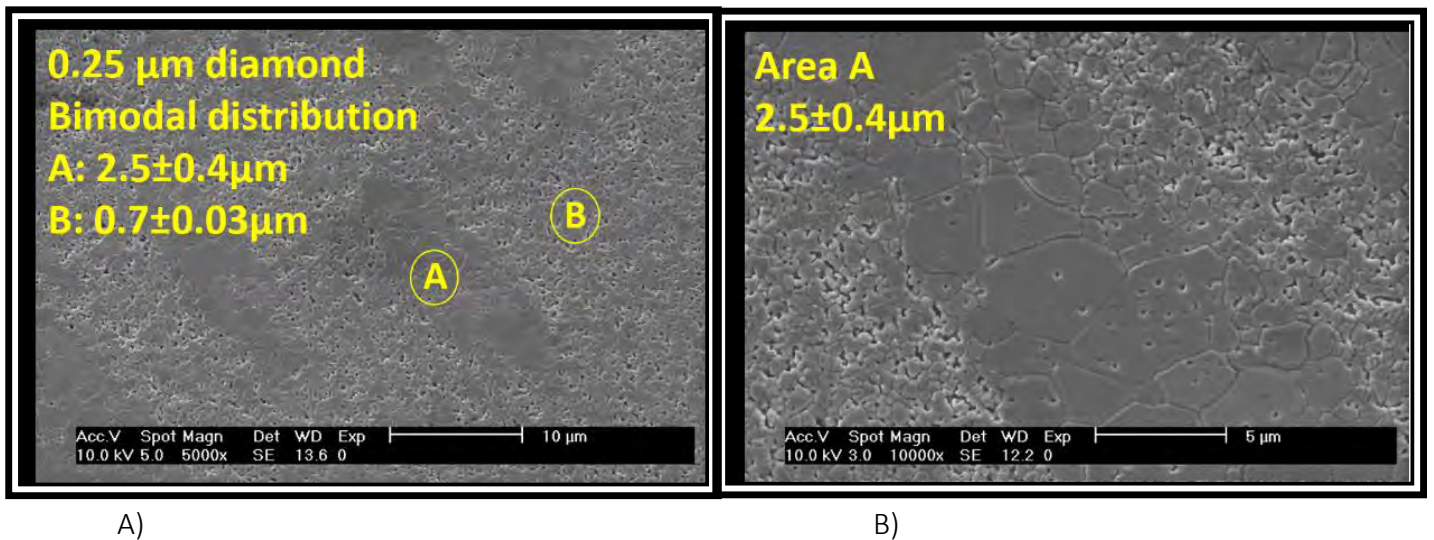
recommended for fabrication of  $UO_2$ -diamond composite pellets.

Figure 2 - XRD spectra of starting powder and  $UO_2$ -70 vol% diamond pellets sintered at various temperatures. Note that formation of UC and graphite phases is revealed at higher temperature.

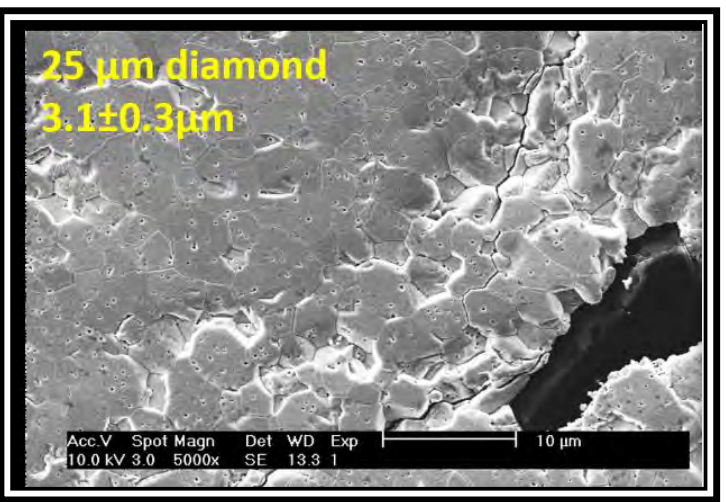
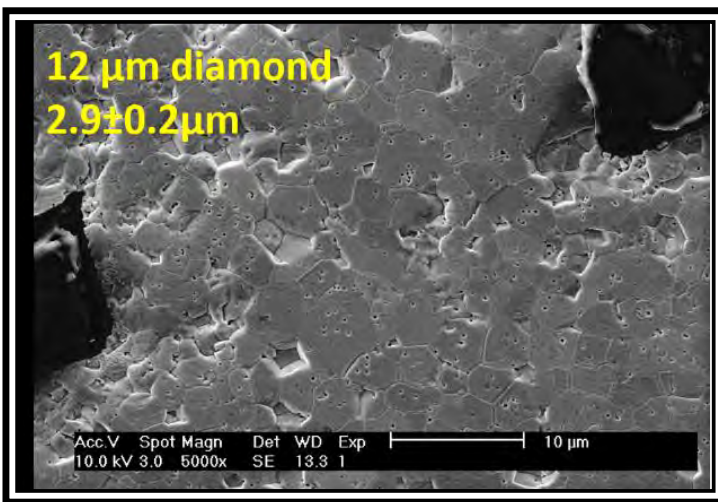
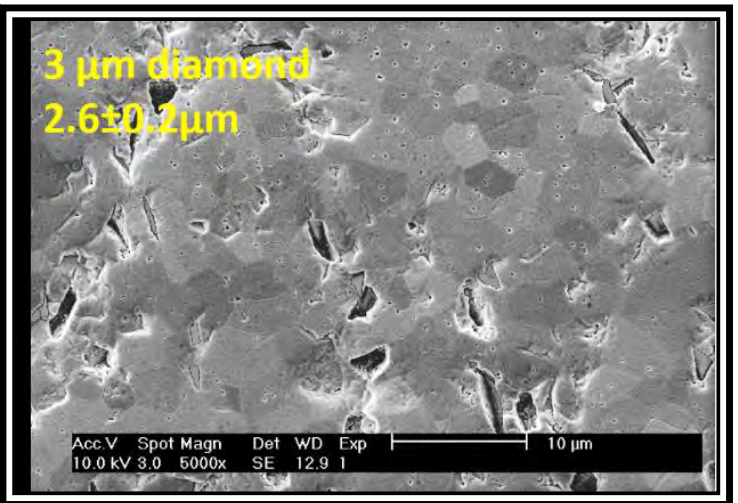
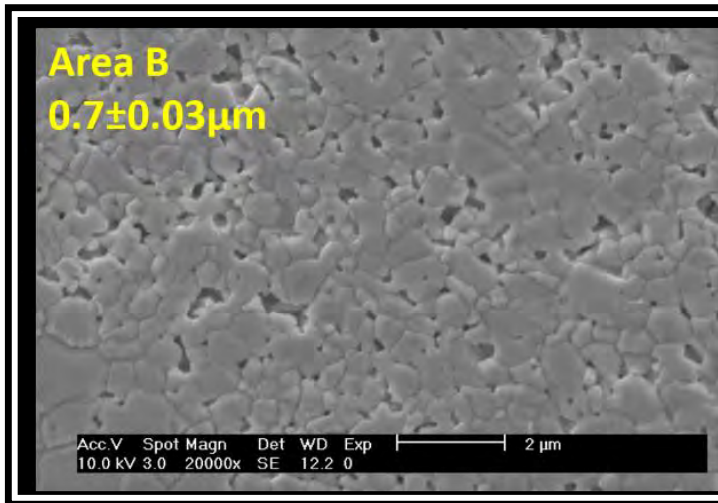
## Grain size

Figure 3 reveals the polished and thermally-etched surfaces of  $\text{UO}_2$ -diamond composite pellets sintered at  $1400^\circ\text{C}$  with a hold time of 5 minutes. Uniform grain sizes were revealed in pellets with  $3\text{ }\mu\text{m}$  diamond (grain size  $=2.6\text{ }\mu\text{m}$ , Figure 3(d)), grain size  $=12\text{ }\mu\text{m}$  diamond (grain size  $=2.9\text{ }\mu\text{m}$ , Figure 3(e)) and  $25\text{ }\mu\text{m}$  diamond (grain size  $=3.1\text{ }\mu\text{m}$ , Figure 3(f)), while an obvious non-uniform grain size distribution was observed in the  $\text{UO}_2$ - $0.25\text{ }\mu\text{m}$  diamond pellet (Figure 3(a)-3(c)). Typical  $\text{UO}_2$  grain sizes were no larger than  $3.5\text{ }\mu\text{m}$  in all these microstructures. However, in the work of Ge et al<sup>4</sup>, it was shown that the grain size of  $\text{UO}_2$  pellets sintered by SPS can be as large as  $8.9\text{ }\mu\text{m}$ , much larger than the current  $\text{UO}_2$  grain sizes in  $\text{UO}_2$ -diamond composites. The results are reasonable when the pinning effect of second phase particles are considered. During sintering, the  $\text{UO}_2$  grains start to grow and once the grain boundary reaches a diamond particle, the grain boundary migration was pinned by that particle. Therefore, smaller grains were formed in the  $\text{UO}_2$  matrix.

Since the volume fraction of diamond is the same in all composites, a higher surface to volume ratio of diamond particles exists in composite containing smaller diamond particles. Therefore, the intensity of pinning effect would be more in composite with  $0.25\text{ }\mu\text{m}$  diamond. It can be seen that within these four  $\text{UO}_2$ -diamond composites, the pellet with  $25\text{ }\mu\text{m}$  diamond particles has the largest grain size, which is in agreement with the above argument.







C)

D)

E)

F)

Figure 3 - Polished and thermally etched surfaces of UO<sub>2</sub>-diamond composites with different mean diamond particle sizes. A) 0.25 μm, D) 3 μm, E) 12 μm, and F) 25 μm. B) and C) are enlarged pictures of areas in A). The grain sizes are indicated on the top left of each image.

## Thermal Conductivity

The measured diffusivity is converted to thermal conductivity by the following relationship:

$$k = \rho \alpha c_p$$

where  $\rho$  is the measured density of the sample,  $\alpha$  is the measured thermal diffusivity, and  $c_p$  is the specific heat of the sample. Since UF has not verified the heat capacity of the pure diamond powder and diamond composite pellets, the specific heat is approximated using rule of mixing for the known literature values for  $\text{UO}_2$  and for diamond. According to work completed at UF using SiC and at TAMU using BeO, the rule of mixtures was used for approximating the specific heat for thermal conductivity results of 10 vol% composite pellets. These results are shown in Figure 4, along with diamond composite thermal conductivity. It shows a 200%, 400%, and 460% increase in thermal conductivity at 100 °C, 500 °C and 900 °C for the 10 vol% diamond composite pellets, a 45-60% increase for the 10 vol% SiC composite pellet and a 60-75% increase for the 10 vol% BeO composite pellet.

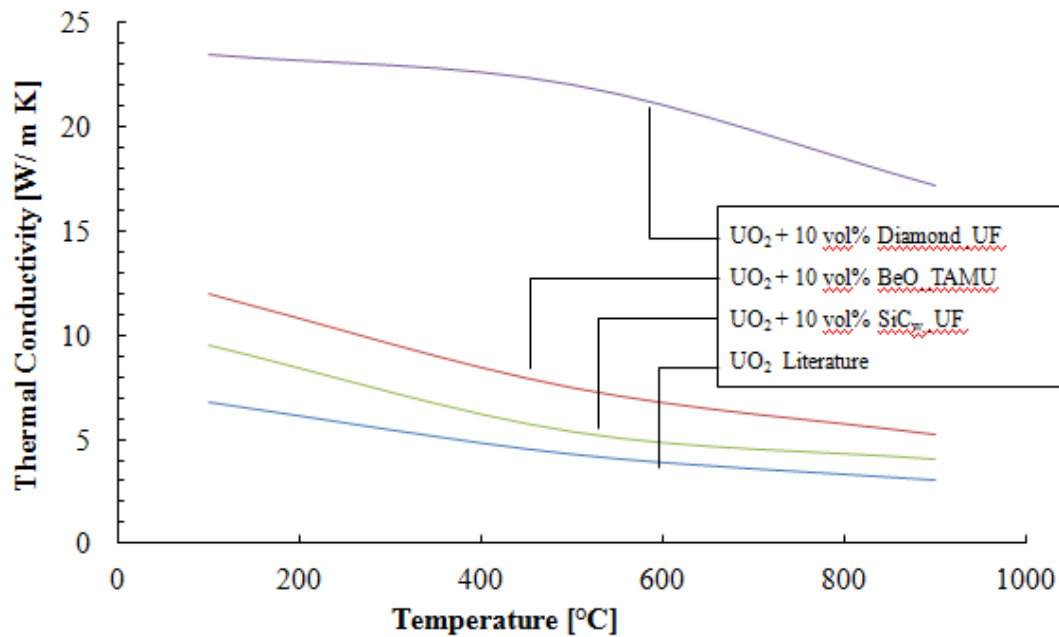


Figure 4 - Thermal Conductivity of Composite Pellets.

## Thermal Conductivity measurements from Los Alamos National Lab (LANL) and Idaho National Lab

UO<sub>2</sub> diamond doped fuel pellets were sent to Los Alamos National Laboratory (LANL) for thermal analysis. LANL measured the thermal diffusivity of the composite pellets by means of a laser flash technique. The thermal conductivity was calculated using the thermal diffusivity measurements

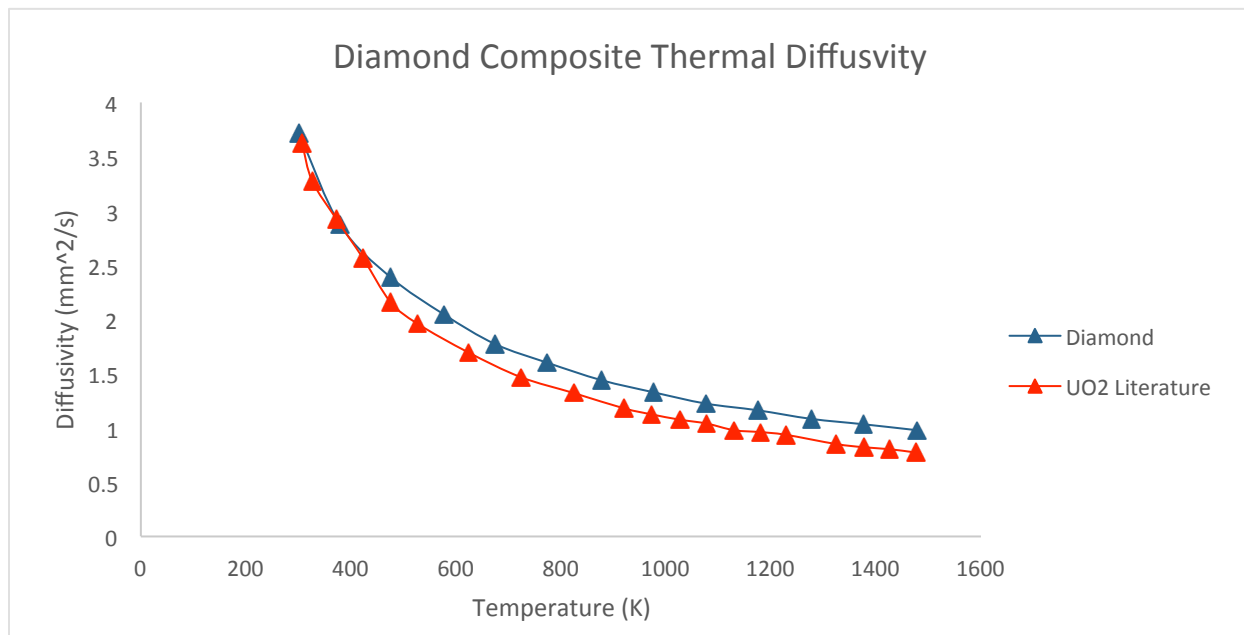


Figure 5a - Thermal Diffusivity data from LANL for diamond composite and literature UO<sub>2</sub>.

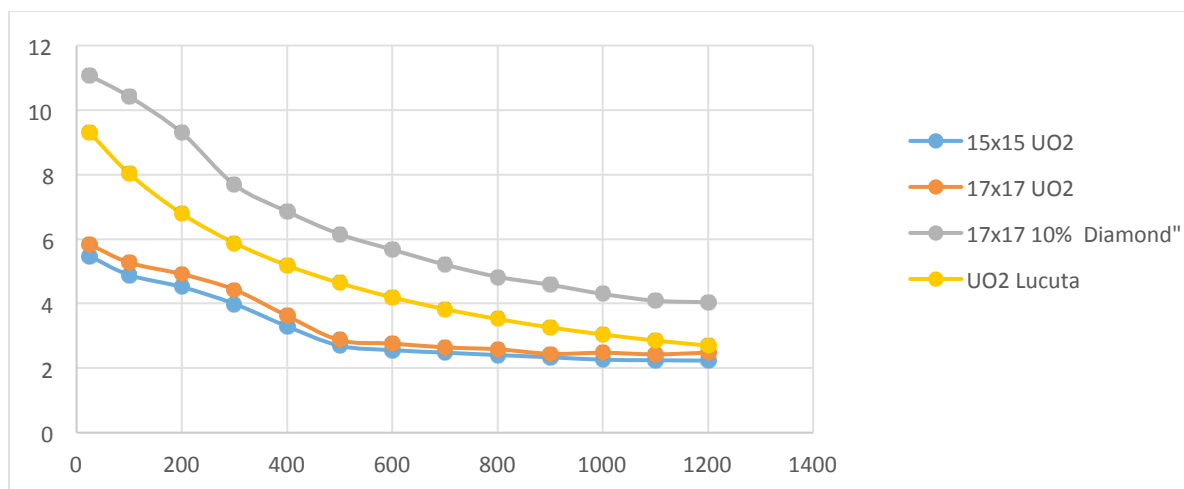


Figure 5b - Thermal Diffusivity data from INL for diamond composite and pure  $\text{UO}_2$ . and literature  $\text{UO}_2$ .

provided by LANL In Figure 5a where the measured thermal diffusivity of the diamond composite pellets is being compared with literature values for  $\text{UO}_2$ . Since the values were considerably lower than the UF measured values samples pellets were sent to INL which measure a considerable improvement of the diamond composite over the  $\text{UO}_2$  in line with the UF measurements. In addition, the thermal conductivity was calculated by using the thermal diffusivity data provided along with measured densities and literature heat capacity values. The heat capacity of the composite was calculated from the component heat capacities through the rule of mixtures. The density calculated for these samples was 96.5 % theoretical density. Thermal conductivity is simply the product of density, heat capacity, and thermal diffusivity. Simultaneously FRAPCON was used to model the in-reactor behavior of the diamond composite pellet developed at UF. The resulting thermal conductivity of the composite pellets is being plotted with respect to the FRAPCON model of  $\text{UO}_2$  and shown in Figure 6.

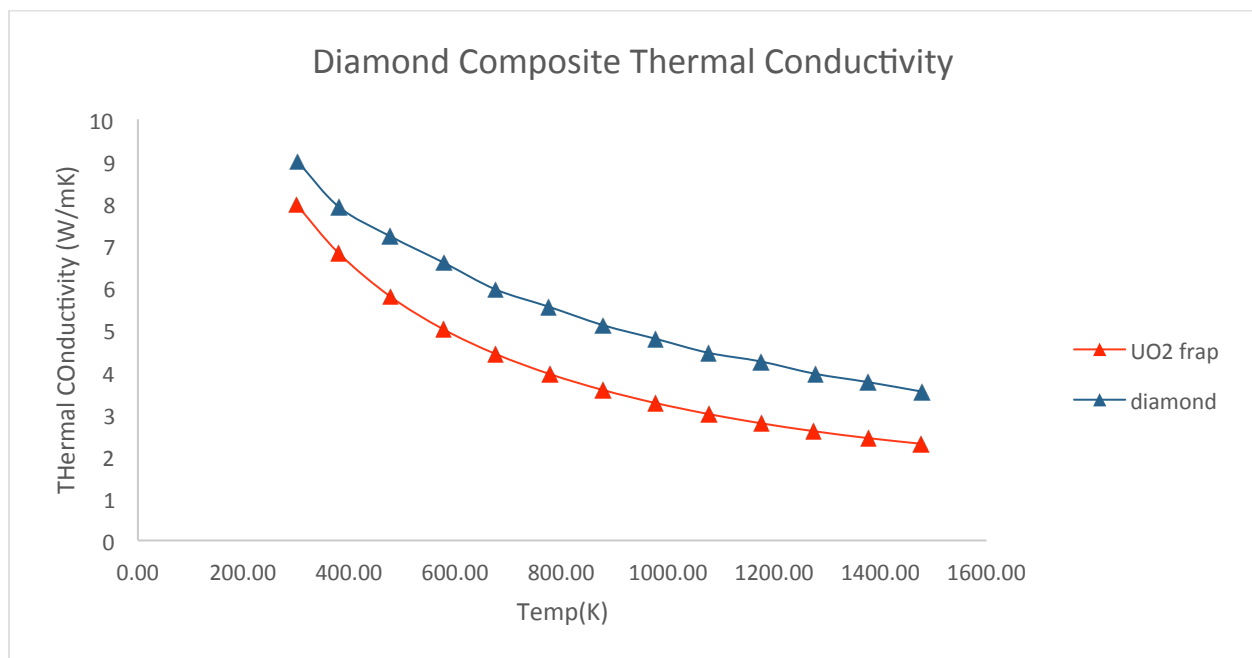


Figure 6 - Calculated diamond thermal conductivity vs Literature  $\text{UO}_2$

The thermal conductivity of diamond pellets was then modelled using the model in FRAPCON. The model used in FRAPCON includes burnup degradation of thermal conductivity; however, the results presented here lacked this unique behavior. The temperature dependence of diamond composite pellets was merged with the burnup dependence of  $\text{UO}_2$  pellets intrinsic to the FRAPCON model. As expected, these results ensure that the modelled thermal conductivity does tend to degrade. Figure 7 shows a comparison of thermal conductivity of  $\text{UO}_2$  diamond doped fuel measured from samples fabricated at UF and compares it with various  $\text{UO}_2$ -based composites. Based on the results, the diamond composite fuel fabricated at UF seems to have a higher thermal conductivity when compared to other  $\text{UO}_2$  based composites.

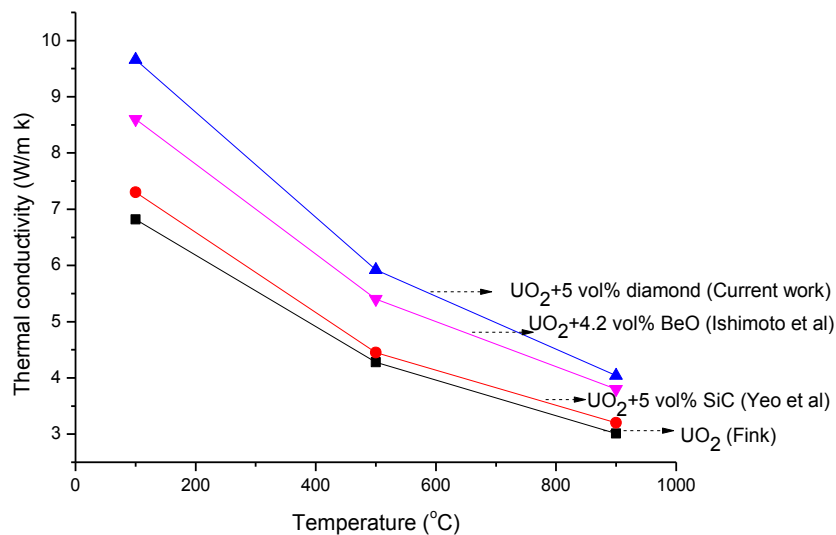


Figure 7 - Comparison of thermal conductivity of  $\text{UO}_2$  and various  $\text{UO}_2$ -based composites

### Age - Wear Test of $\text{UO}_2$ – Diamond Composites Aging Test

The objective of the age/wear test was to check the integrity and change of mechanical and thermal properties for composite fuel pellets after long time exposure to high temperatures. The conditions for the test were a temperature of 1400 °C for a 10 hour hold time. The atmosphere was composed of Argon gas with 1 ppm  $\text{O}_2$ . The heating/cooling rate was set at 2.6 °C/min for a total furnace utilization time of 27 hours. Figure 8 shows an image of the experimental set up for

the Age/Wear Test. Three diamond composite pellets were aged, all containing 1 micron sized diamond powder as the secondary particle. They were 1%, 5%, and 10 vol% composite pellets with densities of 97.0%, 95.6%, and 93.4% TD, respectively. Figure 9 illustrates the pellets after the age test, showing the pellets remain fully dense and intact.

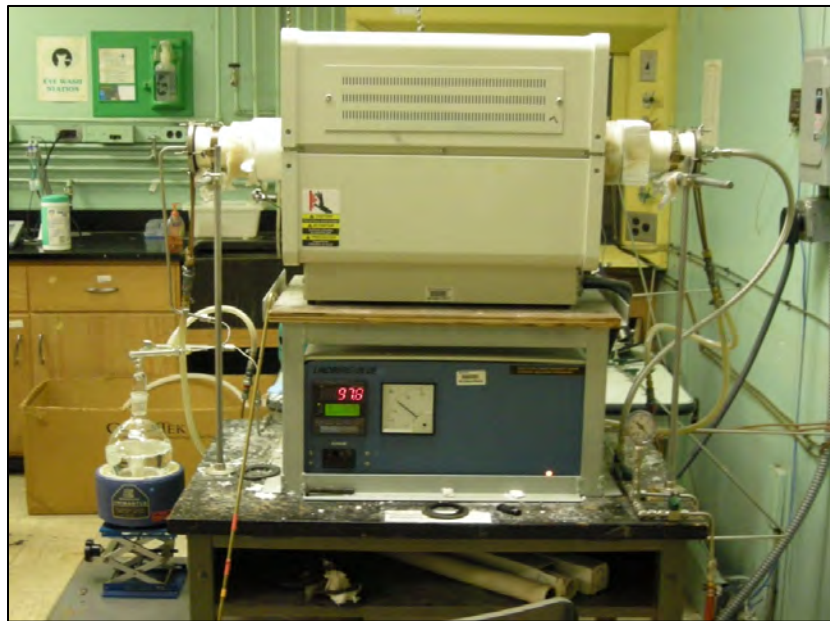


Figure 8 - Tube furnace used for Age/Wear test

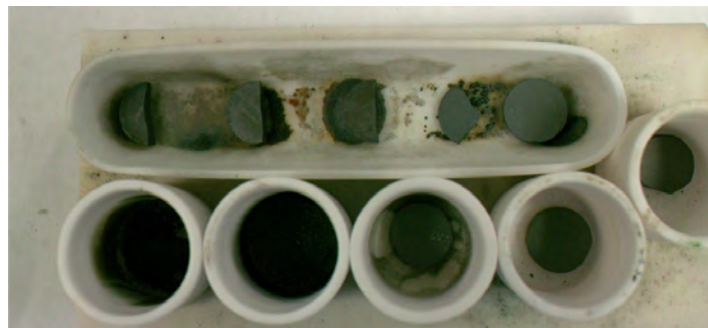


Figure 9 - Diamond composite pellets after aging test

Figures 10-11 show the exterior of a 5 vol% diamond composite pellet before and after aging, which shows that most diamond particles on the surface are removed during the test. However, after fracturing the pellet and examining the interior of the pellet it shows that the diamond particles remain in good interfacial contact with the  $\text{UO}_2$  matrix, Figure 12.



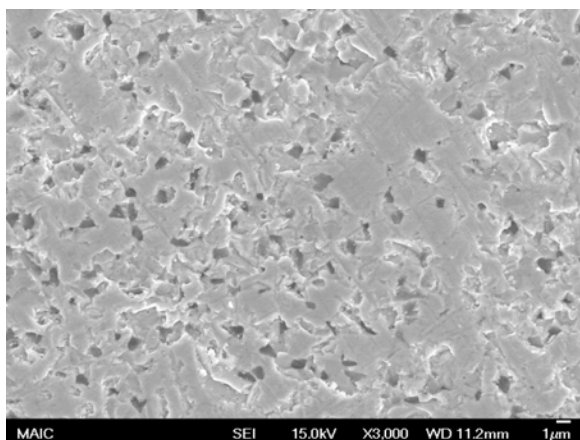


Figure 10- Before Age/Wear Test

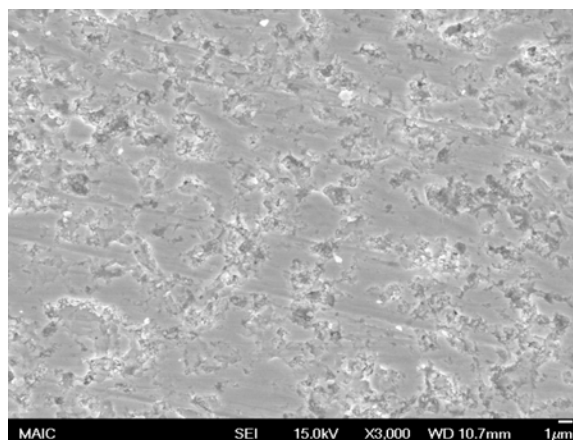


Figure 11 - After the age/wear test

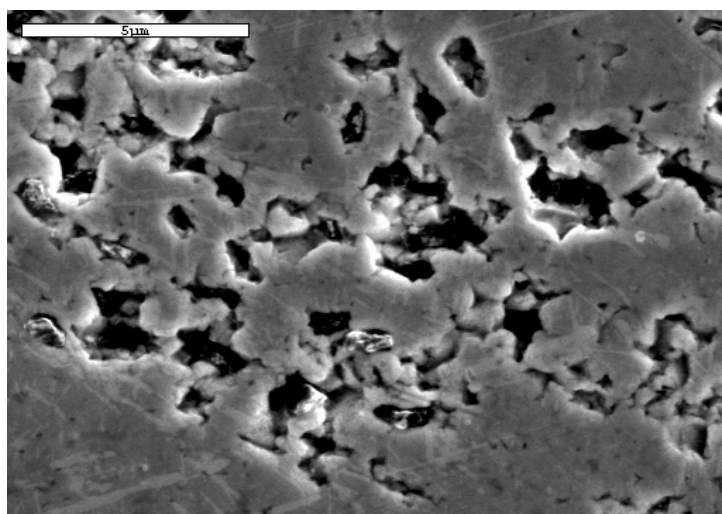


Figure 12 - Interior of fractured diamond composite pellet after aging test

The results of the age/wear test show the  $\text{UO}_2$ -diamond composite pellets can survive at  $1400^\circ\text{C}$  for 10 hours. The diamond particles on the surface may have been oxidized by the 1 ppm  $\text{O}_2$  in the Argon gas, while the interior remains unchanged. Figure 13 also illustrates the thermal diffusivity change is negligible after the age/wear test.

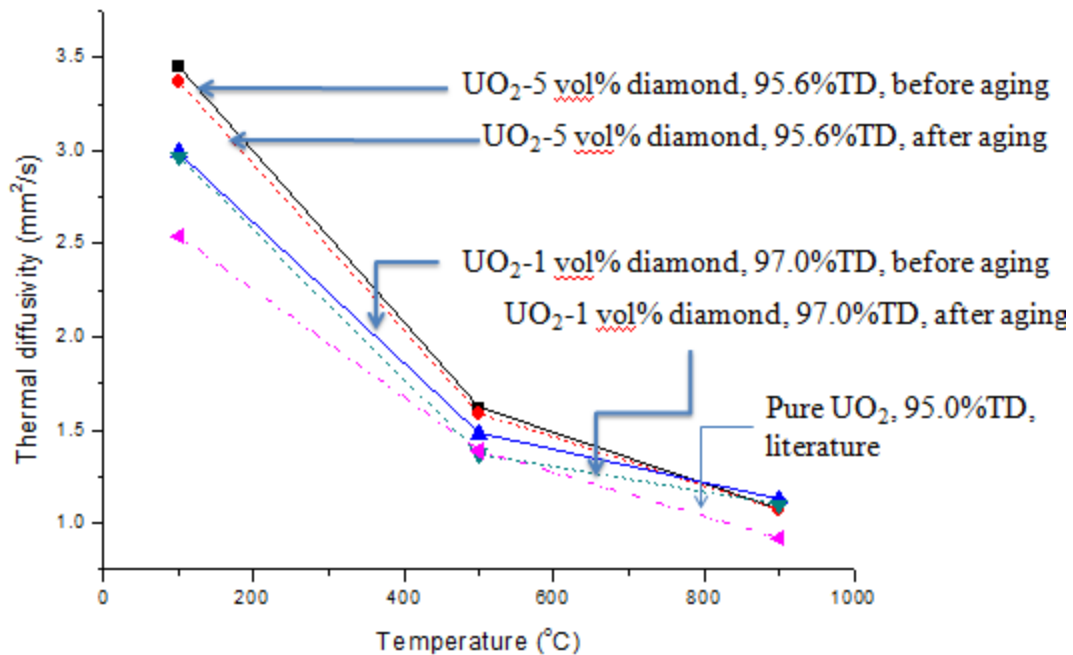


Figure 13 - Thermal diffusivity change due to aging test

## Simulation/Modeling

Initial calculations and simulation of a diamond doped fuel with a relatively minor thermal conductivity increase were run using FRAPCON 3.4. The initial results show the benefit of establishing a higher thermal conductivity fuel pellet into an existing LWR. The FRAPCON fuel performance code was modified to simulate a higher thermal conductivity for the fuel over its lifetime. A test rod for the Br-3 reactor was chosen to demonstrate the thermal property enhancements for the composite fuel pellets. Results for a 17% thermal conductivity show an 8.4% decrease in fuel centerline temperature for the hottest node, and a 4.41% decrease in fission gas release by the end of life. These results only take into account a 17% overall increase in fuel thermal conductivity. CASMO results, in Figure 14, show the difference in dopant fuel reactivity with the change in reactivity (multiplication factor) as a function of burnup.



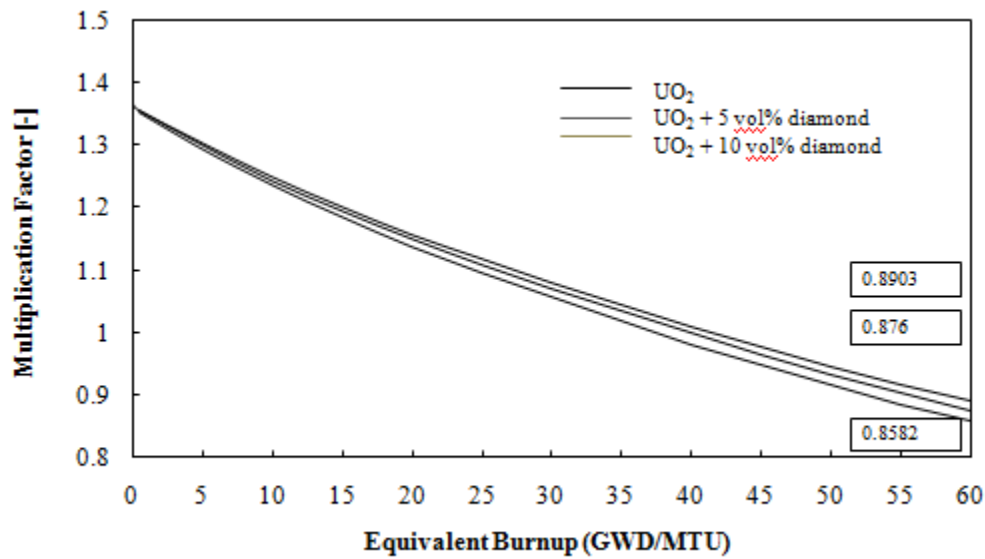


Figure 14 - CASMO4 results for diamond composite pellets with reduced uranium loading.

### Gamma Irradiation Test on UO<sub>2</sub> Diamond doped fuel

UO<sub>2</sub> diamond doped pellets were examined under a gamma radiation environment. The fuel samples were irradiated using a Cs-137 source with an exposure rate of 3384.58 rad/min. The irradiator used was a “JL Shepherd Model 35-14”. Three different samples of ID: A1, A2, and A3 were placed in the irradiator for a period of 72 hours. After removal from the irradiator the micro structure of the samples was analyzed under SEM imaging. The experiment was conducted to analyze alterations at the interfaces, grains, changes in the diamond particles, and any other potential grain defects caused by gamma radiation. The samples evaluated after irradiation did not present any noticeable micro-cracks, porosities, or alterations caused by the gamma irradiation. Figure 15 depicts sample A2, a 12 µm diamond powder 10% volume composite pellet where the interfaces do not show any significant alterations.

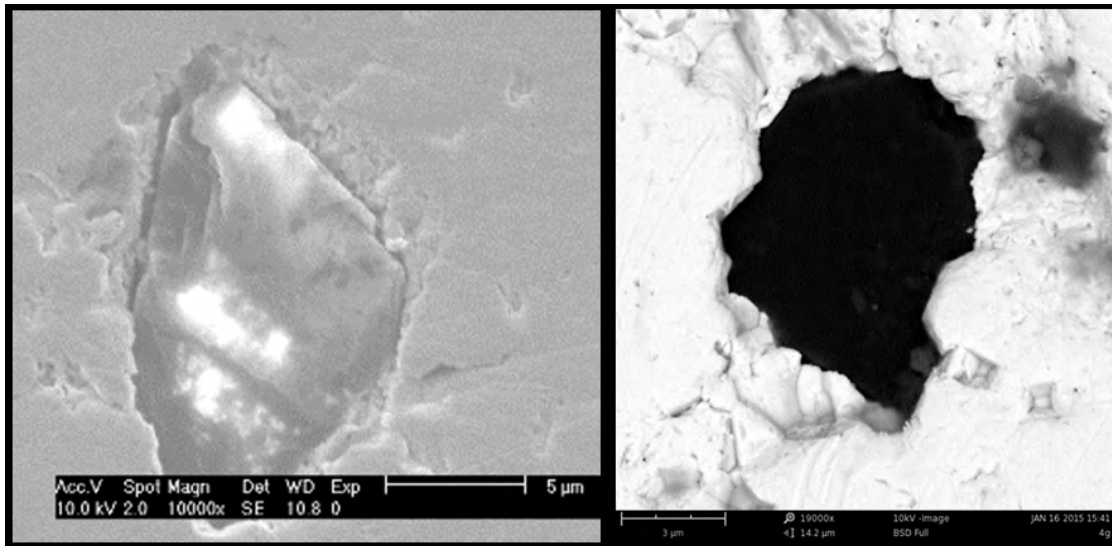


Figure 15 - . Sample A2 before irradiation (left) and Sample A2 after removal from irradiator after 72 hours (right).

In addition, the appearance of micro-cracks in all samples remain constant after removal from the irradiator. It is assumed that the origin of the micro-cracks comes from the sintering process inside the SPS chamber. Figure 16 illustrates sample B2, a 99.94%  $\pm$ theoretical density  $\text{UO}_2$  pellet sintered at 1,450 °C for 5 minutes, where the presence of micro-cracks was uniform throughout the

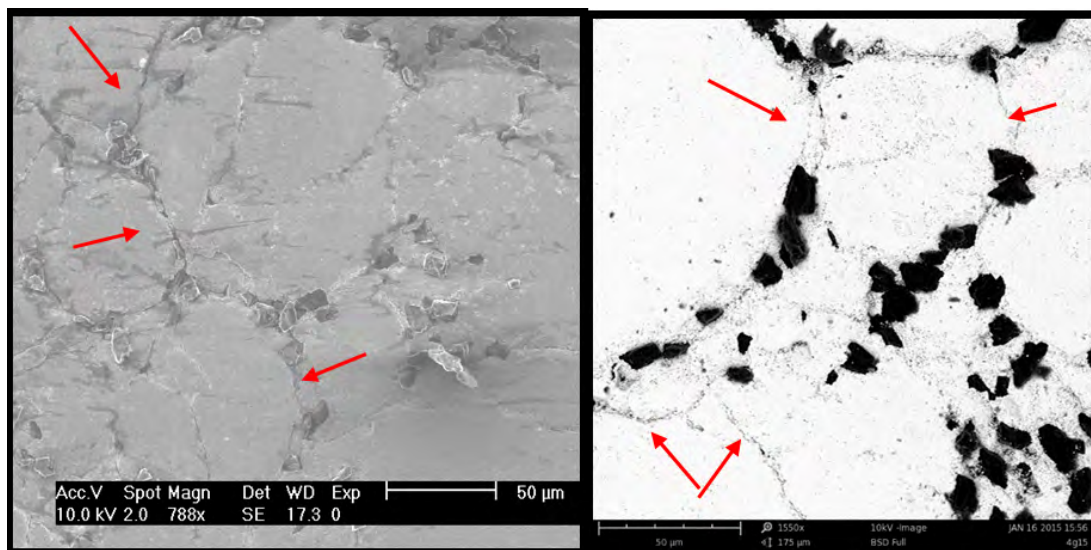


Figure 16 - Sample B2 before irradiation (left) and Sample B2 after removal from irradiator after 24 hours (right). Micro-cracks present before and after irradiation

surface of the pellet. There were no alterations found on the micro-cracks after completion of the 24 hour irradiation test.

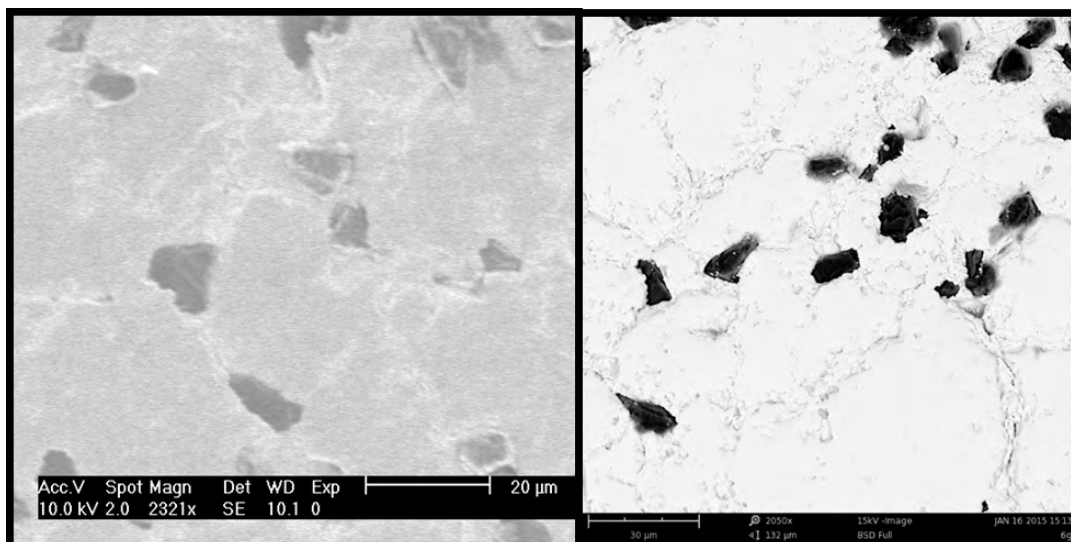


Figure 17 - Sample B1 before irradiation (left) and Sample B2 after removal from irradiator after 24 hours (right). Micro-cracks present before and after irradiation

A non-uniform dispersion of diamond particles into the  $\text{UO}_2$  matrix was found in the samples. The diamond particles remain in a fair interfacial contact with the  $\text{UO}_2$  matrix. Figure 17 shows sample B1, where the diamond particles remain in good contact with the  $\text{UO}_2$  matrix. No irregularities, porosities or other defects were observed throughout the evaluation. The study proved that the gamma source exposure rate was not strong enough to produce noticeable defects or structural changes to the  $\text{UO}_2$  diamond doped samples.

### Young's Modulus

While analyzing the Young's Modulus, which is characterized by the ratio of stress to strain, our study showed that pellets with 3  $\mu\text{m}$  diamond particle size display a higher Young's modulus than pure  $\text{UO}_2$  samples, while pellets with 0.25  $\mu\text{m}$ , 12  $\mu\text{m}$ , and 25  $\mu\text{m}$  diamond showed relative lower values. The reason of this difference can be explained by the microstructure of the pellets. Figure 18 clearly displays that pellets with 3  $\mu\text{m}$  diamond particle have a higher Young's Modulus when compared to other particle sizes. Such claim is in agreement with microstructural studies on diamond and the  $\text{UO}_2$  matrix. Since, the  $\text{UO}_2$ -diamond composite shows better

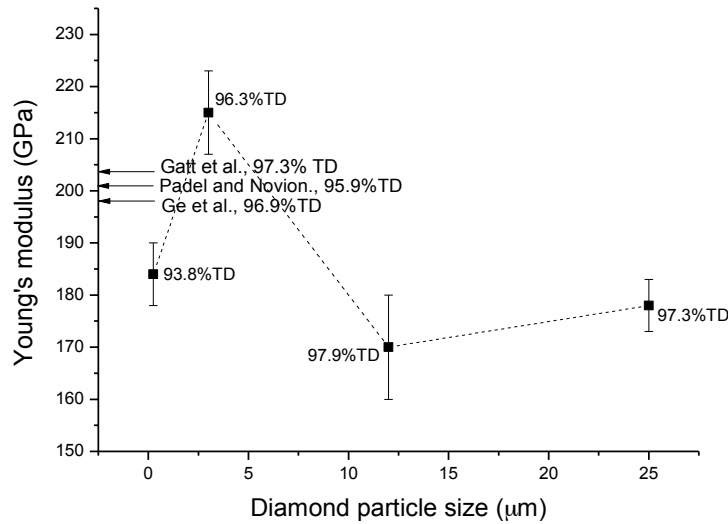


Figure 18 - Young's modulus of UO<sub>2</sub>-5 vol% diamond composites. Arrays represent the Young's modulus of pure UO<sub>2</sub> pellets reported from literature.

thermal conductivity than other UO<sub>2</sub> composites, we have concluded that diamond is a potential candidate to elaborate high thermal conductivity UO<sub>2</sub> composite fuel.

### Variational Diamond Volume Fraction Analysis

Experimental work was performed to analyze the grain size and relative density of UO<sub>2</sub> composites with a variation on the diamond volume fraction. The sintered compacts were studied systematically for their microstructure including grain size, shape, porosity, and interfacial structure between UO<sub>2</sub> and diamond particles. The UO<sub>2</sub> powder was doped with diamond micro-particles at 5%, 10%, and 15% diamond volume fraction with a diamond particle size of 3 μm. During the sintering process the axial pressure was set to 40 MPa with a hold time of 3 minutes. Temperatures of 1000 °C, 1200 °C, and 1400 °C were evaluated to find an optimal parameter for each composite volume fraction.

Since fuel performance is dependent on the thermal conductivity of the fuel, and since the thermal conductivity is proportional to the density of the fuel<sup>5</sup>, it is believed that the later

parameter is also being maximized. Each of the varying volume fraction samples was sintered at three different peak temperatures. The selected temperatures were 1000 °C, 1200 °C, and 1400 °C. During sintering the heating rate remained constant at 100 °C per minute for all samples. After completion of the sintering process, the samples were polished and thermally etched prior to being analyzed under SEM. The grain size was calculated by the line interception method on the axially cut samples. Grain size and other microstructural properties greatly influence the total relative density and the thermal properties of the manufactured pellets.<sup>6</sup>

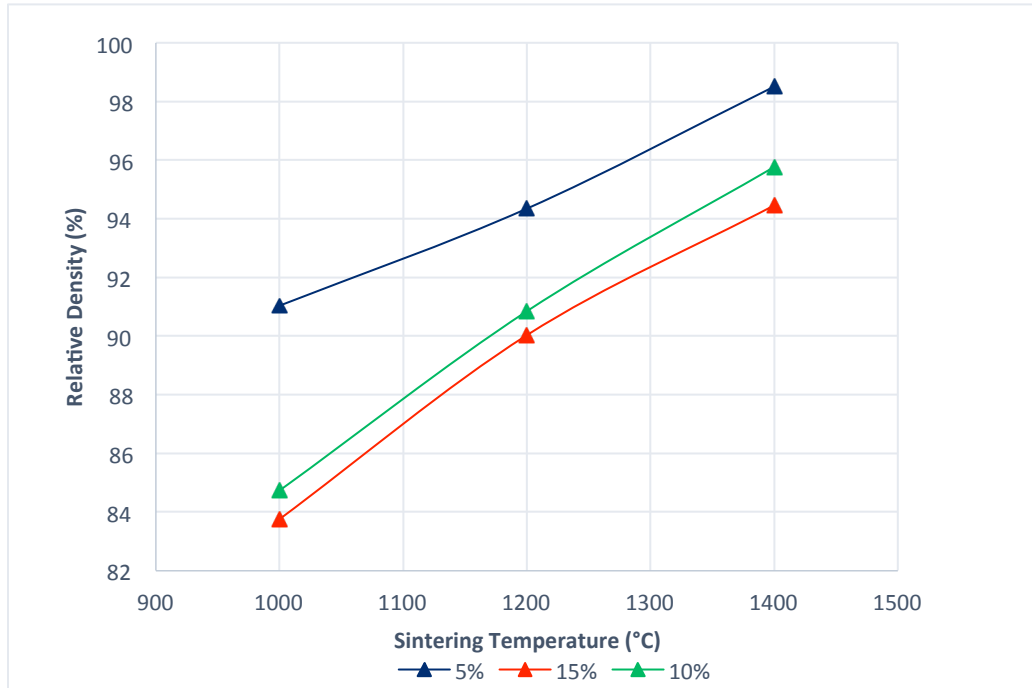
The analysis showed that the UO<sub>2</sub> samples displayed higher densities as the volume fractions of diamond were being reduced. The grain size, which is a crucial factor influencing the density, was found to increase proportionally with peak sintering temperature. In addition, it was confirmed that the smallest diamond volume fraction showed the highest densities at all sintering temperatures. Table 1 shows the relative densities along with their respective sintering temperature and diamond volume fraction. As expected, the increase in sintering temperature assisted in the densification of the samples.

Sintering Temperature	Diamond 5% Vol	Diamond 10% Vol	Diamond 15% Vol
1000 °C	91.03 %	84.71 %	82.80 %
1200 °C	94.34 %	90.85 %	90.03 %
1400 °C	98.51 %	95.77 %	94.46 %

Table 1- Relative densities from UO<sub>2</sub> samples with different diamond volume fractions sintered at different temperatures.

The samples sintered at the highest peak temperature displayed the highest densities. The analysis performed by Bobrovnitchii et al. confirms that the sintering temperature has a strong impact on the density of the fuel.<sup>7</sup> Figure 19 clearly exemplifies the behavior of the temperature regimes on the different diamond volume fractions evaluated. The 5% diamond volume fraction samples showed the highest densities, while the 15% diamond volume fraction samples showed the lowest. This inverse relationship between composite volume fraction and relative density may be explained by the fact that diamond particles create a solid boundary to UO<sub>2</sub> grains within

the sample's lattice. As a result, the grain growth of  $\text{UO}_2$  was affected, limiting densification. It can be assumed that at higher concentrations of diamond powder a higher sintering



temperature will be required to completely densify and improve the thermal properties.

Figure 19- Relative densities plotted with respect to the sintering temperatures for different diamond volume fractions.

The microstructural analysis displayed grain sizes ranging from  $0.57 \mu\text{m}$  to  $2.53 \mu\text{m}$  while sintered at the three different temperature gradients. Table 2 shows how the grain sizes increased as a function of the sintering temperature. As determined by the experimental work of Ge et al, increasing the sintering temperature enhances the grain growth process, reduces porosities, and increases the density of samples<sup>6</sup>. The findings of Ge et al. were confirmed in this experiment. Figure 20 shows the grain size of the samples with 5% diamond volume fraction. It can be clearly seen that the relative sample grain size increases as a function of the sintering temperature.

Sintering Temperature	Diamond 5% Vol	Diamond 10% Vol	Diamond 15% Vol
1000 °C	0.89	0.57	0.56
1200 °C	1.12	1.03	1.1
1400 °C	1.82	2.44	2.53

Table 2- Evaluated grain sizes of samples with different diamond volume fractions sintered at different temperatures.

Figure 20 (c) shows the greatest grain size, and corresponds to the sample with the highest relative density (98.51%). Figure 21 displays the temperature effects on the grain size. At a sintering temperature of 1400°C all of the volume fractions present their largest grain size. The grain size dependence on the diamond concentration displayed an inconsistent behavior based on the samples examined. Additional research work will be conducted in order to arrive at an understanding of such behavior.

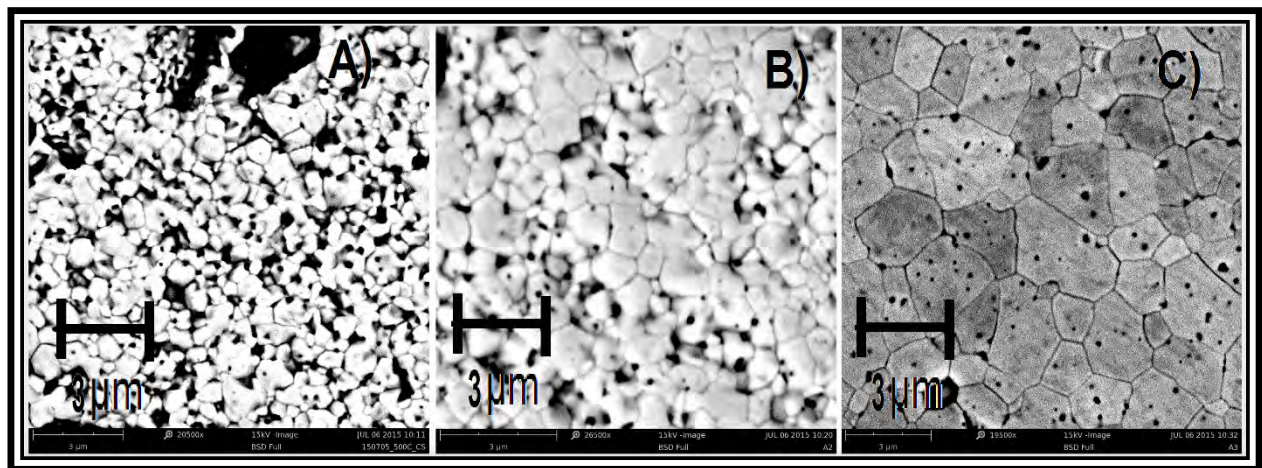


Figure 20- SEM images of samples with diamond volume fraction of 5%. A) Sintering temperature of 1000°C and grain size 0.89 µm. B) Sintering temperature of 1200° and grain size 1.12 µm. C) Sintering temperature of 1400° and grain size 1.82 µm.

In order to increase the grain growth in our fuel, different sintering parameters with low heating rates and long hold times were tested along the sintering process. However, it still remains a subject of future research work at UF. The density and microstructure analyses showed that a

strong relationship exists between the diamond volumetric fraction and the relative densities. As the diamond powder concentration increases, the densification of the samples ceases.

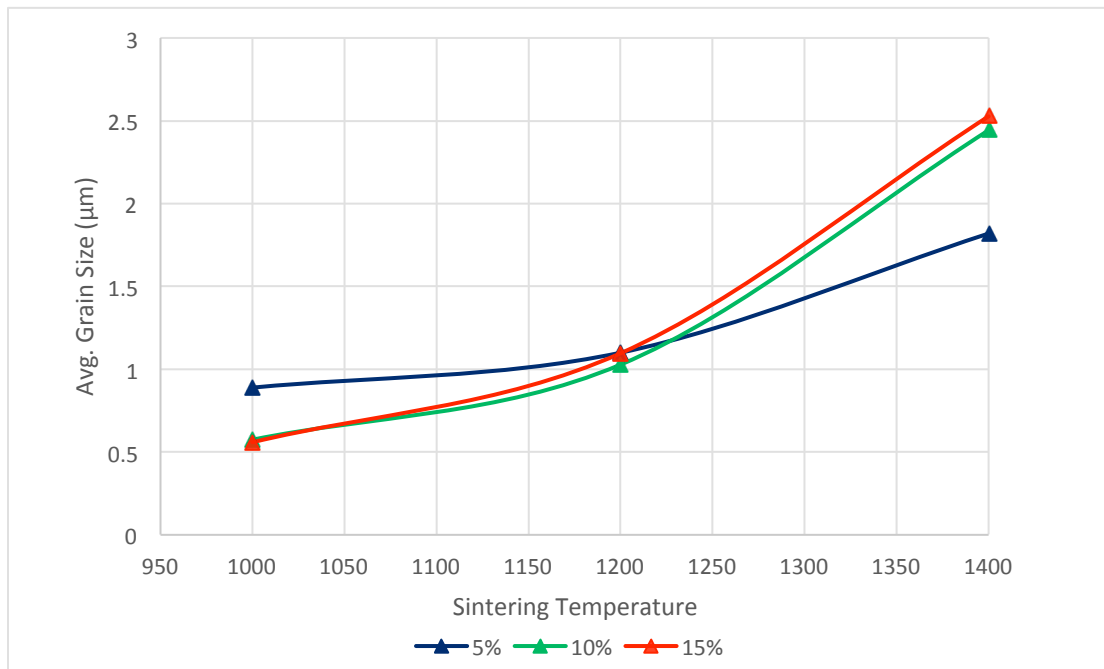


Figure 21 - Average grain size of different diamond volume fractions with respect to their sintering temperature.

The grain size's dependence on the diamond concentration was not possible to extrapolate from the data. The behavior seemed fairly unpredictable based on these results but further studies will need to be performed to understand the relationship. The peak sintering temperature was also found to be a strong determinant of relative density. In all samples examined, an increase in sintering temperature resulted in an increase in relative density. This was further reaffirmed in the microstructure analysis, where a positive relationship between the sample grain sizes and sintering temperatures was found.



## SPS production of full size UO<sub>2</sub> Diamond pellets

The objective of producing full size fuel pellets was to arrive at an optimum parameter to manufacture UO<sub>2</sub> diamond doped fuel with a high density while meeting the industry dimensions. The industry dimensions recommended by AREVA LLC consisted on a pellet length of  $10.16 \pm 1.27$  mm, diameter of  $8.19 \pm 0.025$  mm, and a relative density of 96.5% or higher. Different configurations with variations in hold time, sample weight, and temperature were tested. Table 3 depicts the different sintering parameters used for the fuel fabrication process.

Sample ID	Weight(g)	Length(mm)	Diameter	Relative Density	Hold Time	Temp	Pressure	Heating
				(%)				Rate
R1	4.85	10.58	8.13	87.27	1 min	1000	40 Mpa	100°/min
R2	4.89	10.19	8.11	91.92	1 min	1200	40 Mpa	100°/min
R3	4.87	10.56	8.13	87.67	3 min	1000	40 Mpa	100°/min
R4	4.80	9.84	8.16	92.06	3 min	1200	40 Mpa	100°/min
D1.1	5.31	10.07	8.19	98.76	5 min	1400	40 Mpa	100°/min
D2.1	5.52	10.51	8.21	98.14	5 min	1400	40 Mpa	100°/min
D1.2	5.62	10.92	8.19	96.36	5 min	1400	40 Mpa	100°/min
D2.2	5.63	10.78	8.21	97.38	5 min	1400	40 Mpa	100°/min
D1.3	4.62	8.81	8.18	98.32	5 min	1400	40 Mpa	100°/min
D1.4	5.51	10.93	8.21	94.07	5 min	1400	40 Mpa	100°/min

D2.3	5.51	10.48	8.21	98.21	5 min	1400	40 Mpa	100°/min
D2.4	5.61	10.78	8.21	96.99	5 min	1400	40 Mpa	100°/min
D1.5	5.67	11.13	8.18	95.65	5 min	1400	40 Mpa	100°/min
UF1	5.15	10.04	8.17	96.57	5 min	1400	40 Mpa	100°/min

Table 3 – Sintering parameters employed for UO<sup>2</sup> diamond doped fuel fabrication

The sintering parameters for samples R1 through R4, was initially set at temperatures of 1,000 and 1,200 degrees Celsius with a heating rate of 100°/min and an axial pressure of 40 Map. The heating rate and axial pressure remained constant for all configurations. Initially, the sintering hold time was evaluated at 1 minute for samples R1 and R2 with peak temperatures of 1000°C and 1200°C respectively. But the relative density and pellet diameter were not meeting the requested criteria. The hold time was increased to 3 minutes for samples R3 and R4 and a slight increase in relative density was noticed. However, at these configurations some of the samples were not fully sintered. This issue was being reflected on the low relative density and microstructure presented. To achieve a high density the temperature was increased to 1400°C and the hold times were extended to 5 minutes, reaching density values close the theoretical density of the compound. Samples R1 through R4 were fabricated using a die with an inner diameter (ID) of 0.322 in ~ 8.17 mm. However, the produced pellet's diameter was not up to the specified standards. Thus, a different die with an ID of 0.325 in ~ 8.25 mm was used to obtain a radius of the desired dimensions. The later die of 0.325 was used to complete samples D1.1 through UF1. At this configuration 10 consecutive samples were fabricated and the die wear was analyzed.

During the pellet fabrication process two dies were subject to wear analysis. Figure 22 shows the dies' mass loss as the dies are used in different sintering runs.

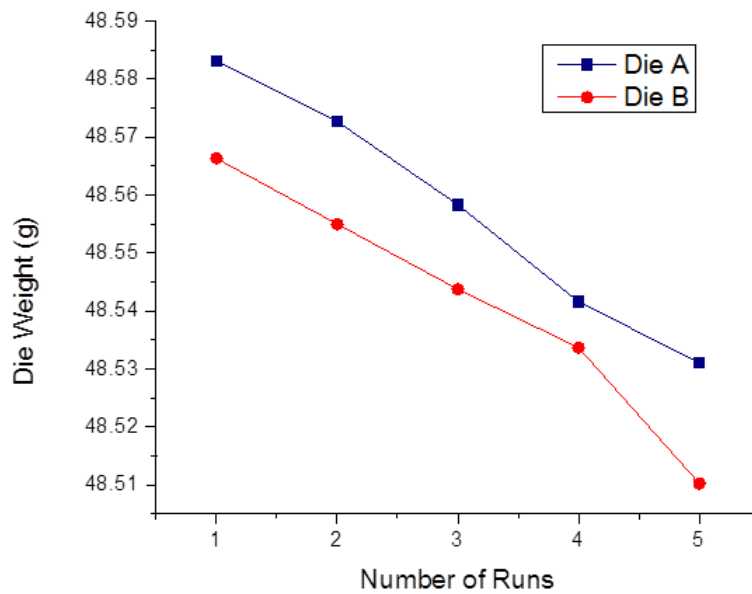
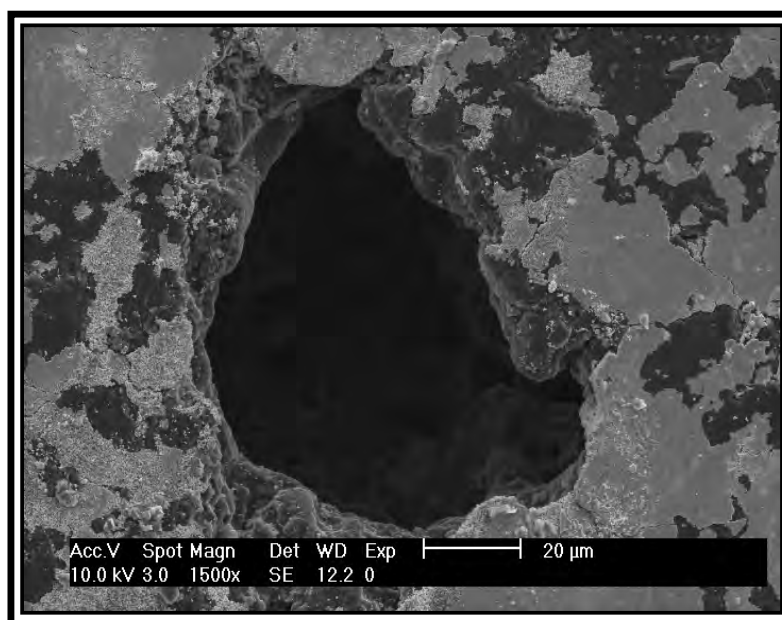


Figure 22- Mass loss of graphite dies during different sintering runs

The average mass loss per sintering run was calculated to be  $15 \pm 3.14$  mg, which represents 0.03% of the initial mass of the die. It was concluded that most of the mass was lost while extracting the sintered pellet. As the pellet is being pushed along the die, the die experiences friction forces leading to scratches and holes. Figure 23 clearly shows one of several voids found



along the die wall.

Figure 23 – Void accumulation at the die wall

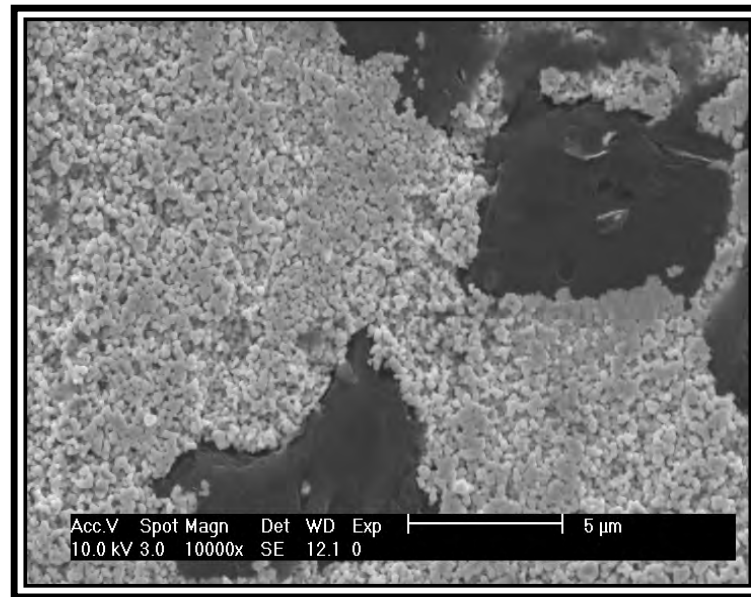


Figure 24 –  $\text{UO}_2$  inclusions found at the die inner wall.

The accumulation of voids has caused dies to experience fracture due to brittleness during the sintering process. Besides void formation, while analyzing our dies under SEM,  $\text{UO}_2$  inclusions were found at the inner surfaces. The inclusions were generated during the sintering process. As the temperatures increase, the  $\text{UO}_2$  powder sinters and attaches to the wall of the die. Figure 24 illustrates the inclusions found on the dies after various sintering runs. Along the manufacturing process UF has incorporated dish and chamfer on the pellet production. Dish and chamfer at the end of the pellet allows room for fission gas products to accumulate. In addition, the dish and chamfer geometries carry the least stress on the pellet when compared to other geometry designs.<sup>8</sup> Figure 25 shows full size pellets with dish and chamfer produced by SPS. All samples have enhanced thermal properties, high relative densities, and acceptable dimensions for use in LWRs.

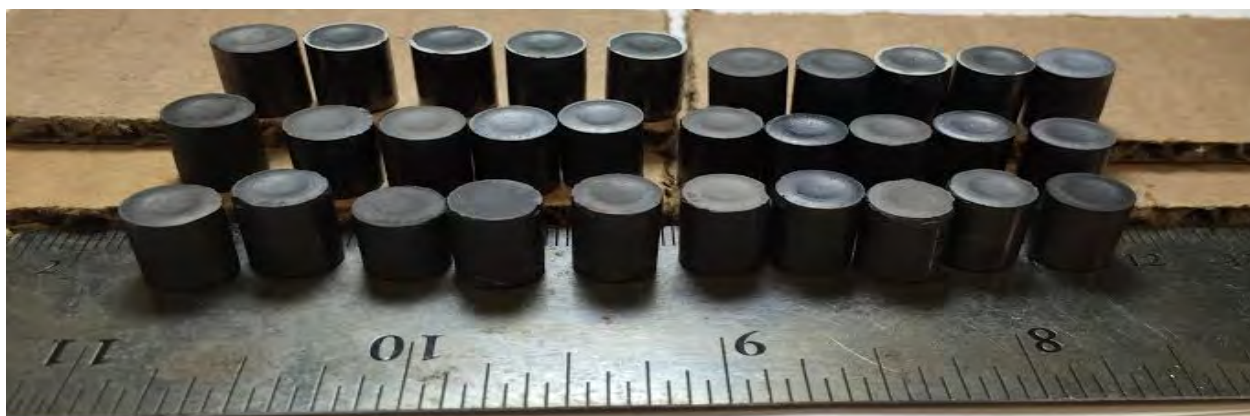


Figure 25 –  $\text{UO}_2$  full size pellets with dish and chamfer produced via SPS.

#### **Production of $\text{UO}_2$ -Diamond composite fuel pellets for ATR**

$\text{UO}_2$  with a 4.95% enrichment was doped with diamond particles for the fabrication of fuel pellets. Such pellets are being irradiated at the Advanced Test Reactor (ATR) at the Idaho National Laboratory facility to verify the maintenance of the increased thermal conductivity of the Diamond-composites fuel. The fabrication of the 17X17 small diameter fuel pellets presented challenges not encountered with the 15X15 larger diameter fuel pellets. The challenges presented were chipping and cracking on a large majority of the samples. Figure 26 displays an image of a diamond doped fuel pellet produced for the ATR reactor. Chipping was present and several cracks were encountered at both surfaces. The use of a graphite punch to manufacture the dish at the surface of the pellet may exacerbate or even create these issues. Table 4 shows the number of samples created for the irradiation study along with the mean theoretical density with its respective standard deviation. We are currently awaiting on the irradiation results from the ATR at the Idaho National Laboratory facility.

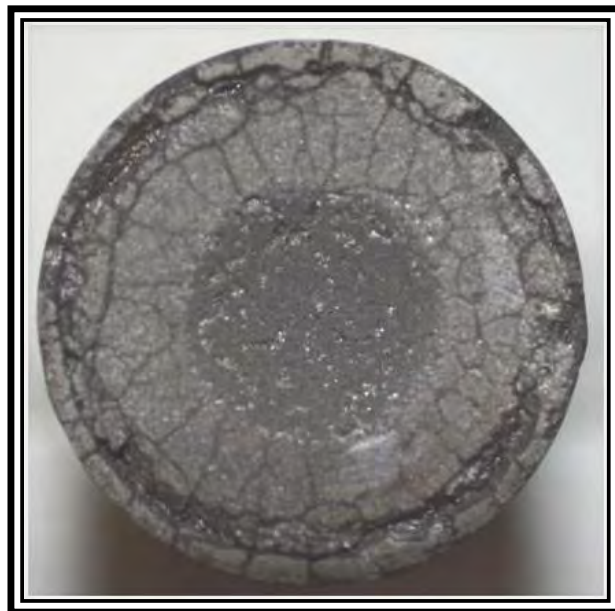


Figure 26 - ATR Diamond Composite Pellet edge

<b>Number of samples measured</b>	21
<b>Sample Mean %TD</b>	95.4 %TD
<b>Standard Deviation</b>	0.709 %TD
<b>95% Confidence Interval</b>	(95.0 %TD, 95.7 %TD)

Table 4 – ATR fuel sample fabrication relative density

### **Economic Analysis**

SPS batch processing is projected as being only 15% of the total processing cost compared to conventional sintering procedures, not including cost of materials and the facility, labor or post processing expenses. Processing via SPS also allows for increasing profitability even further by net shaping (minimal or no secondary machining). This net shaping provides not only a unique technical advantage, but also potentially a significant economic advantage over traditional methods of fuel fabrication which require centerless grinding. Traditional sintering processes take upwards of 8 to 12 hours or more to reach completion plus also require an initial powder pressing step to approximately 60% density prior to sintering. Conversely, utilizing SPS, a batch of pellets can be fabricated in as little as 10 minutes. Batch production involves fabricating more than one sample at a time during SPS process. To perform the economic analysis, it was assumed that during each run, 12 samples were fabricated. In order to quantify the effect SPS batch processing has on the nuclear fuel cycle, several basic assumptions were made to simplify the calculations. The cost of electricity was set at \$0.12/kW-hr, the national average in 2013. The cost of each die/punch unit was \$3000. The furnace was operating for 6 days a week, 24 hours a day. The 7th day of the week will be utilized for equipment maintenance including the replacement of the dies/punches. The sample cycle time was increased to 15 minutes to allow for die loading and unloading. Utilizing the power consumption measured at UF and the assumptions outlined above, the total power draw of the 12 batch setup was projected as 8461 kW-hr. Running 6 days a week for a month, this power

consumption was projected to cost approximately \$24,368. Factoring the cost to replace the graphite dies, this total come out to \$36,368 per month to run this batch setup. A total of 2304 batches will be produced yielding 27, 648 pellets. This brings the total cost of fabrication, not including capital cost and cost of fuel material or enrichment, to be ~\$1.32/pellet.

## **Conclusion**

The concept of high thermal conductivity UO<sub>2</sub>-diamond composite fuel pellets has been demonstrated. Using the spark plasma sintering technique, UO<sub>2</sub>-10 vol% diamond composite fuel pellets were successfully sintered and proved to meet the industry's dimensions and thermal properties for reactor performance. A maximum sintering temperature of 1400°C and a hold time of 5 minutes are recommended in order to achieve a high density pellet with minimal UO<sub>2</sub>-diamond chemical reaction. Four diamond particle sizes ranging from 0.25 µm to 25 µm were investigated. However, pellets with 0.25 µm diamond particles were not acceptable due to the poor mixing and the resulting low densification. On the other hand, micro-cracks were observed when the diamond particle size was larger than 12 µm, which adversely influenced both the thermal and mechanical properties of the composites. Therefore, a 3 µm diamond is recommended for the UO<sub>2</sub>-diamond composite pellet in order to obtain the best thermal and mechanical performance.

For the UO<sub>2</sub>-diamond composite pellets, the maximum increase in thermal conductivity was found to be 41.6%, 38.3% and 34.2% at 100°C, 500°C and 900°C, respectively. These results are higher than those reported in literature for other UO<sub>2</sub>-based composites. After successfully meeting the industry standards, along with compression tests and thermal properties measurements, diamond proves to be a strong candidate for UO<sub>2</sub> composite fuel pellets. However, further analysis of fuel performance during reactor operation will be performed and will allow collect more experimental data to validate diamond as a potential dopant for accident tolerant fuel.

## **References**

- 1- Chen, Z. (2015) "Densification evolution and properties evaluation of UO<sub>2</sub> based composites prepared by spark plasma sintering" University of Florida, Gainesville.

- 2- Rudajevová A, von Buch F, Mordike BL: Thermal diffusivity and thermal conductivity of MgSc alloys. *Journal of Alloys and Compounds* 1999, 292(1–2):27-30.
- 3- Davies G, Evans T: Graphitization of diamond at zero pressure and at a high pressure. *Proceedings of the Royal Society of London Series A, Mathematical and Physical Sciences* 1972:413-427.
- 4- Ge L, Subhash G, Baney RH, Tulenko JS: Influence of processing parameters on thermal conductivity of uranium dioxide pellets prepared by spark plasma sintering. *Journal of the European Ceramic Society* 2014, 34(7):1791-1801.
- 5- R. Asamoto, F. Anselin, and A. Conti, J. Nucl. Mater. 29, 67 (1969)
- 6- L. Ge, G. Subhash, R.H. Baney, J.S. Tulenko, E. McKenna : Densification of uranium dioxide fuel pellets prepared by spark plasma sintering (SPS). *Journal of Nuclear Materials*. 435 (2013) 1–9.
- 7- G. Bobrovnitchii, O. Osipov, International Journal of Refractory Metals and Hard Materials. Vol 21. 5-6 (2003)251
- 8- International Atomic Energy Agency. *Advanced fuel pellet materials and designs for water cooled reactors* - IAEA-TECDOC-1416 - Nuclear Fuel Cycle and Materials Section. Vienna, Austria. October 2004